Polymer 50 (2009) 2716–2726

Contents lists available at ScienceDirect

Polymer

journal homepage: www.elsevier.com/locate/polymer

Self-organized ordered microporous thin films from grafting copolymers

Wenyong Liu [a,b], Ruigang Liu [a,*], Yanxiang Li [a,b], Wen Wang [a,b], Lin Ma [a,b], Min Wu [a], Yong Huang [a,c,*]

[a] State Key Laboratory of Polymer Physics and Chemistry, Beijing National Laboratory for Molecular Sciences, Institute of Chemistry, Chinese Academy of Sciences, Beijing 100190, China
[b] Graduate University, Chinese Academy of Sciences, Beijing 100039, China
[c] Laboratory of Cellulose and Lignocellulosics Chemistry, Guangzhou Institute of Chemistry, Chinese Academy of Sciences, Guangzhou 510650, China

ARTICLE INFO

Article history:
Received 14 November 2008
Received in revised form
19 March 2009
Accepted 3 April 2009
Available online 12 April 2009

Keywords:
Ordered microporous
Honeycomb
Graft copolymer

ABSTRACT

Highly ordered porous films of cellulose-based graft copolymers were prepared by the breath figure method upon solvent evaporation. The morphology of the microporous films was investigated by scanning electron microscopy (SEM) and atom force microscopy (AFM). The influences of the preparing conditions, the length and the type of the side chains of copolymers on the morphology of the porous films were investigated. It was found that the average pore size is decreased with increasing the concentration of copolymer solutions and with increasing the side chain length. Moreover, it was confirmed that both the present aggregation in solution and the timely precipitation of copolymer are beneficial for the formation of the ordered microstructure by comparison of solvent and the property of side chains of copolymers. The porous films can be used as the template for the preparation of the micropatterning of fluorescence materials and have the potential applications in many fields such as templates, devices, nanocontainer, photonic and bandgap materials.

1. Introduction

Microporous films with regular patterned structure have the potential applications for filter membranes, optical materials, catalysts, templates, cell culture substrates, transparent and super hydrophobic polymer films, etc. [1–8] and have received increased interest in recent years. The microporous films can be prepared by various methods, such as lithography [9], colloidal crystal template [10], emulsion droplets template [11], and bio-template [12]. However, these methods have the disadvantages of being complicated, expensive, and are unable to control the pore size dynamically [13,14]. Recently, simple methods based on the self-organized or self-assembly process of polymers have been developed to prepare patterned micropore and attracted increasing interests for fabricating the film microstructure [15–18]. Among these methods, the so called "breath figures" method first reported by Francois et al. [18,19] is the most attractive one, due to its facility to fabricate the ordered porous films.

The mechanism of the formation of the ordered structure by this method and the preparation of ordered microporous films have been studied extensively [8,16,20–27]. It is believed that water droplets condensed from water vapor acted as the templates for the ordered arrays. During this procedure, the surface of the polymer solution was cooled by the evaporation of the volatile solvents, which leads to the condensation of the water vapor onto the surfaces. The polymer was then precipitated and the highly ordered structure was formed. The precipitation rate of the polymer relates to the polymer concentration, the solvent and the polymer that used and is a key factor to this procedure [19]. The published results indicate that the ordered microporous films from different polymers can be prepared by this method [28–37]. Based on the growing published results on this method, the mechanism of this method is still not fully understood due to the complexity of the process [38].

More recently, the use of biocompatible and biodegradable polymers for the fabrication of orderly structures has received much attention because of their advantages for biomedical applications [39,40]. As a kind of naturally renewable, biodegradable and biocompatible polymers, cellulose and its derivatives are attractive in many fields, such as membrane, fiber and porous materials [41–46]. In order to use cellulose and its derivatives more efficiently, the grafting and chemical modification of cellulose and its derivatives have been studied extensively, and cellulose graft copolymers with well-defined architectures have been successfully synthesized by using atom-transfer radical polymerization (ATRP) and reversible addition fragmentation chain transfer polymerization (RAFT)

* Corresponding authors. State Key Laboratory of Polymer Physics and Chemistry, Beijing National Laboratory for Molecular Sciences, Institute of Chemistry, Chinese Academy of Sciences, Beijing 100190, China. Tel.: +86 10 82618573; fax: +86 10 62559373.
E-mail addresses: rgliu@iccas.ac.cn (R. Liu), yhuang@cashq.ac.cn (Y. Huang).

0032-3861/$ – see front matter © 2009 Elsevier Ltd. All rights reserved.
doi:10.1016/j.polymer.2009.04.009

Table 1
Details of the graft copolymers used for the preparation of microporous film.

Copolymers[a]	$M_n \times 10^{-5}$ (g/mol)[b]	M_w/M_n[b]	[Monomer]/[glucose] molar ratio[c]	Average repeat units of side chains (DP)
$EC_{0.5}$-*g*-PS_{256}	1.49	1.32	128	256
$EC_{0.5}$-*g*-PS_{162}	1.34	1.38	81	162
$EC_{0.5}$-*g*-PS_{84}	1.20	1.41	42	84
$EC_{0.5}$-*g*-PS_{20}	1.13	1.47	10	20
$EC_{0.5}$-*g*-$PtBA_{53}$	1.72	1.41	26.5	53
$EC_{0.02}$-*g*-$P(PEGMA)_{57}$	1.42	1.52	1.1	57

[a] The subscript numbers of *m* and *n* in EC_m-*g*-PS_n form represent the number of side chains per glucose unit and the average repeat units of the side chains, respectively.
[b] Determined by GPC.
[c] Molar ratio of average styrene or PEGMA unit and glucose unit was determined by ^1H NMR.

[47–51]. The obtained cellulose graft copolymers have the potential applications in biomaterials, biosensors, filters, etc.

In our previous work, the synthesis and potential application of well-defined cellulosic graft copolymers have been investigated [52–57]. In present work, we report the self-organized microporous structures based on cellulosic graft copolymers. The ordered porous films were prepared by the breath figures method. The dependence of the pore size of the porous films prepared from the comb hydroxypropylcellulose graft polystyrene (HPC-*g*-PS) synthesized via RAFT has been reported [25]. It has been found that the pore size increases with the decreasing concentration of the casting solutions and the increasing of the arm length. Herein the comb cellulosic copolymers with the hydrophobic ethyl cellulose backbone were used to prepare the honeycomb structured porous films. The effects of the relative humidity, solution concentration, graft length, solvent and type of the side chains of the cellulose graft

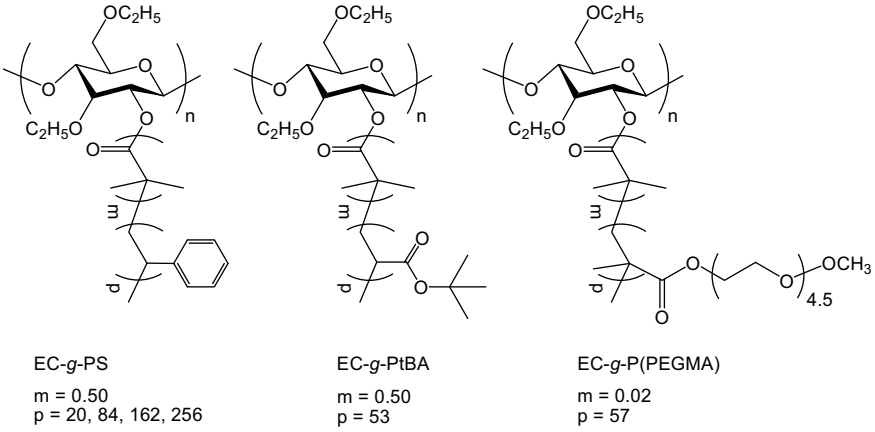

Scheme 1. Molecular structures of the graft copolymers.

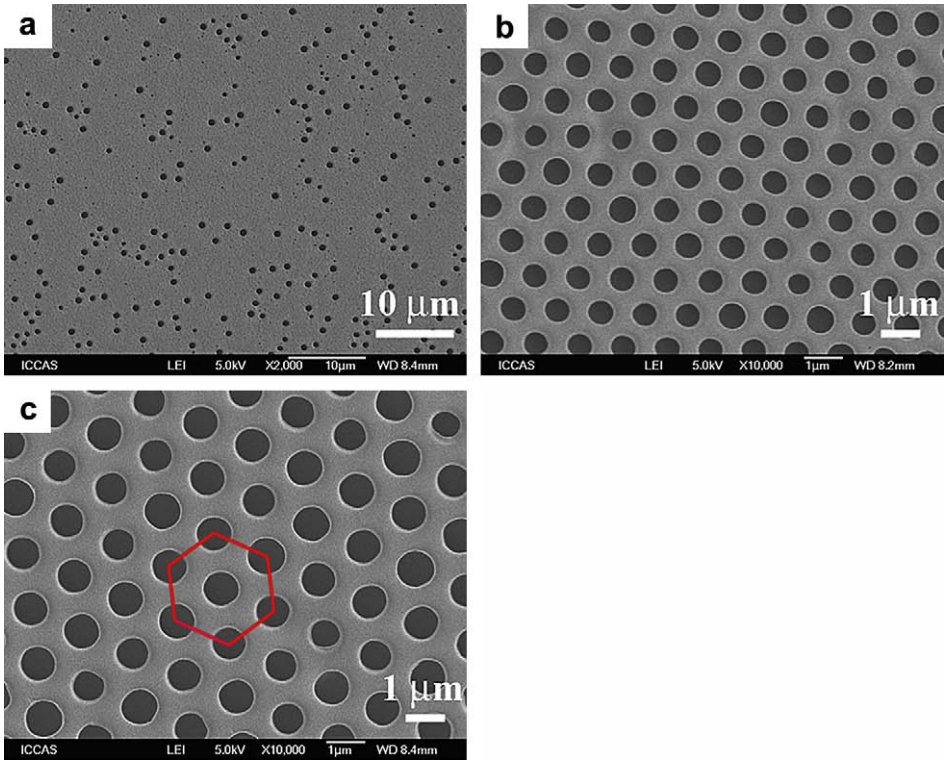

Fig. 1. SEM images of the porous films prepared from 10 g/L copolymer $EC_{0.5}$-*g*-PS_{84}/CS_2 solution at the RH of (a) 30%, (b) 62%, and (c) 72% RH. The hexagonally ordered arrangement of the pores is illustrated by the red line. (For interpretation of the reference to color in this figure legend, the reader is referred to the web version of this article.)

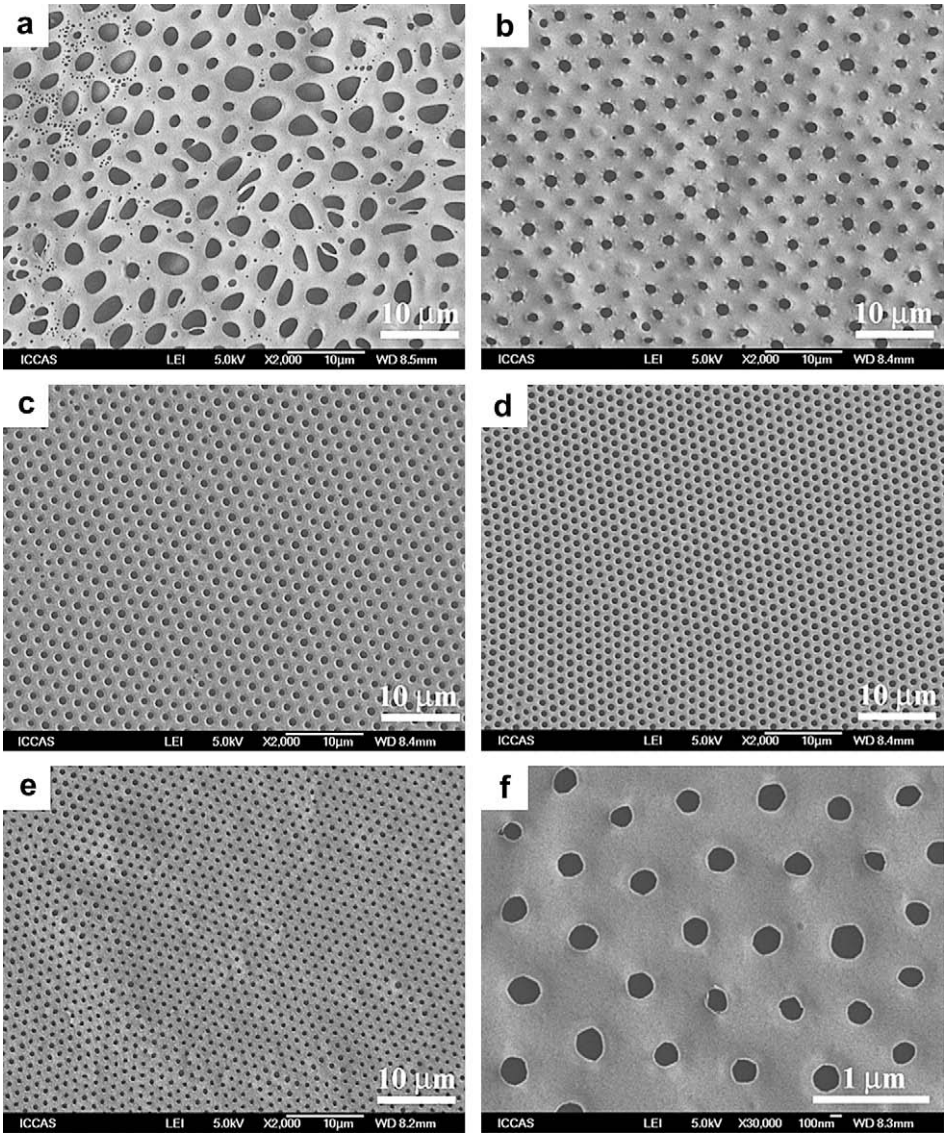

Fig. 2. SEM images of the porous films prepared from copolymer $EC_{0.5}$-*g*-PS_{84}/CS_2 solutions with the copolymer concentration of (a) 1, (b) 2, (c) 5, (d) 10, (e) 15, and (f) 20 g/L at RH of 72%.

copolymers on the microporous structures were investigated systematically. Order patterned fluorescence films can be prepared by the simply hybrid of the copolymer and organic dye. Our results may be helpful for the understanding of the mechanism of the formation of the ordered porous structure of the breath figure method. The films are promising for various applications in template, biomaterial, nanocontainer, optical materials, photonic band gaps, and so on.

2. Experimental section

2.1. Materials

Ethyl cellulose graft polystyrene (EC-*g*-PS), ethyl cellulose graft poly(tert-butyl acrylate) (EC-*g*-PtBA) and ethyl cellulose graft poly-(poly(ethylene glycol) methyl ether methacrylate) (EC-*g*-P(PEGMA)) were synthesized by atom-transfer radical polymerization (ATRP) [54–56]. The molar mass and its distribution of the graft copolymers were determined by gel permeation chromatography (GPC) (Waters 515 with a 2410 differential refractometer detector) with tetrahydrofuran (THF) as the eluting solvent (1 mL/min) and the monodisperse polystyrene was used as the standard. The composition of the copolymer was estimated by ^{1}H NMR spectra measured by a Bruker DMX 400 NMR spectrometer. The details of the EC-*g*-PS copolymers, the EC-*g*-PtBA cpolymer and the EC-*g*-P(PEGMA) copolymer are listed in Table 1 and Scheme 1. Fluorescence dye, oil red O was purchased from Amresco and was used as purchased. Other solvents (analytical reagent) were commercially available and used as received.

2.2. Film preparation and characterization

The cellulose graft copolymers were first dissolved in the solvents at certain concentration, and then the solutions were dropped onto the clean glass slide in a humidity chamber, in which a moister (Yadu, China) was used to control the relative humidity and a hygrometer (Beijing Yaguang Intruments Co., Ltd, China) was used to measure the relative humidity. The obtained films were left to dry before observation. The film for fluorescence imaging was prepared from copolymer solution containing 0.1 wt% fluorescence dye oil red O.

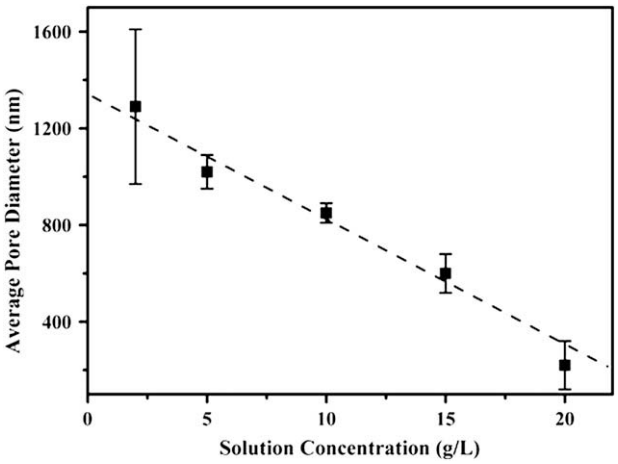

Fig. 3. The average pore size as a function of copolymer concentration of the porous films prepared from $EC_{0.5}$-*g*-PS_{84}/CS_2 solutions at RH of 72%.

Scanning electron microscopic observations were carried out on a scanning electron microscope (JEOL 6700F, Japan) operated at 5 kV and 10 μA. Atom force microscopic (AFM) images were recorded by a Digital Instrument Nanoscope III Multimode system in tapping mode. A silicon cantilever with a bending spring constant of 20–60 N/m and a resonance frequency of about 250–350 kHz was used for imaging at a scan rate of 0.5 Hz. For fluorescence imaging, a Carl Zeiss LSM 510 confocal laser scanning microscope was used and the excitation wavelength of 488 nm was chosen.

Dynamic light scattering (DLS) experiments were performed on a commercial spectrometer (ALV/SP-150) equipped with an ALV-5000 multi-τ digital time correlator and a solid-state laser light source (ADLAS DPY 425 II, output powder was 400 mW at $\lambda = 632.8$ nm). DLS experiments were performed at 25 °C at the scattering angle of 90°. The apparent hydrodynamic radius (R_h) was obtained by the CONTIN program.

3. Results and discussion

In the "breath figure" method, the evaporation of the organic solvent leads to the cooling of the surface of the solution and then the water vapor is condensed into droplet on the solution surface. The water droplets act as the template for the formation of ordered microporous films. Therefore, the relative humidity (RH) of the atmosphere is very important in the procedure and had been investigated extensively [58,59]. Generally, a high RH value is needed for the ordered arrays due to that water droplets act as the templates for the formation of the ordered microporous structure besides the solvent-induced mechanism [17] and the self-assembly in selective solvent [15,60]. Fig. 1 shows the typical SEM images of the films prepared from copolymer $EC_{0.5}$-*g*-PS_{84} ($DP_{St} = 84$) solution in CS_2 at different RH values. The results show that when the solution was cast at the RH of 62% and 72%, the emulsification process occurred and a white film was obtained on the glass substrate, which indicated that the water vapor was condensed on the solution surface. By comparison, no emulsification occurred at the RH of 30% and a transparent film was obtained. Only few porous structures can be observed by SEM from the transparent film (Fig. 1a). Whereas, hexagonally ordered porous structure can be observed by SEM from the white film (Fig. 1(b) and (c)). The results suggest that the distribution of water droplets acted as the templates for the formation of the ordered honeycomb structure in this work. Under low RH atmosphere, no sufficient water droplets were condensed onto the solution surface and the water droplets is too sparse to arrange orderly. Higher relative humidity was required to obtain highly ordered porous thin films. Moreover, it

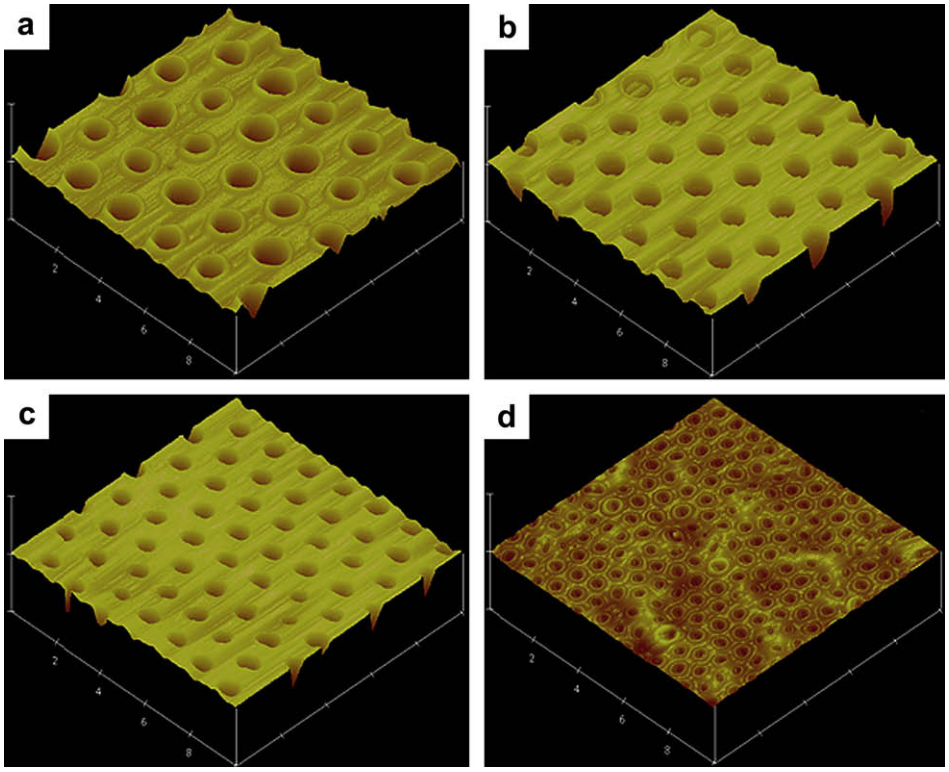

Fig. 4. AFM images of microporous structures of the films prepared from copolymer $EC_{0.5}$-*g*-PS_{84}/CS_2 solutions with the copolymer concentration of (a) 5, (b) 10, (c) 15, and (d) 20 g/L at RH = 72% (*X*, *Y*: 2 μm/div, *Z*: 2 μm/div).

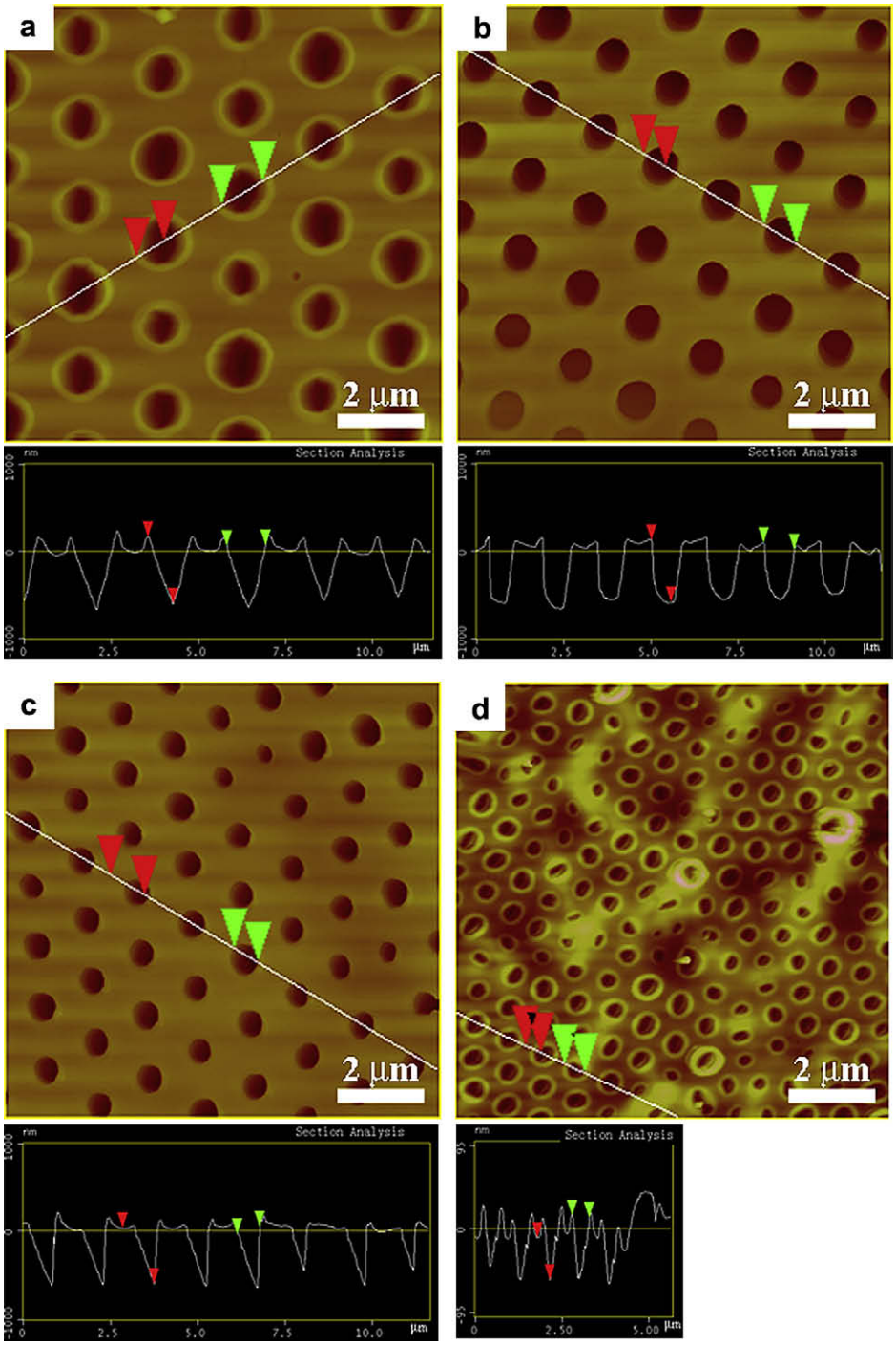

Fig. 5. Top view and cross-sectional analysis of the microporous structures of the films prepared from copolymer $EC_{0.5}$-*g*-PS_{84}/CS_2 solutions with the copolymer concentration of (a) 5, (b) 10, (c) 15, and (d) 20 g/L.

was clearly observed that the pore diameter increased from 620 nm to 850 nm with increasing the RH from 62% to 72%, and this is due to the formation of larger water droplets at higher RH as reported in previous work [61–63]. This means that the pore size from the copolymer could be tailored by altering the relative humidity.

Fig. 2 shows the morphology of the microporous films prepared from copolymer $EC_{0.5}$-*g*-PS_{84}/CS_2 solutions with different polymer concentration. The RH of the atmosphere was adjusted at 72%. The results show that the average pore size of the obtained film decreased from 4.0 μm to 100 nm when the polymer concentration increased from 1 to 20 g/L (Fig. 3). The correlation between pore size and solution concentration is in accordance with literature [25,61–64]. The smallest pore size is similar to the smallest pores reported in literature till to date for this method [65]. Moreover, relatively ordered patterns were obtained in range of copolymer concentration between 2 and 15 g/L, and the most ordered microporous film was obtained at the copolymer of 10 g/L. The pores are in a regular hexagonal arrangement. The pore structures were further confirmed by AFM. The average pore diameters from AFM were consistent with those from SEM as shown in Fig. 4. Using the

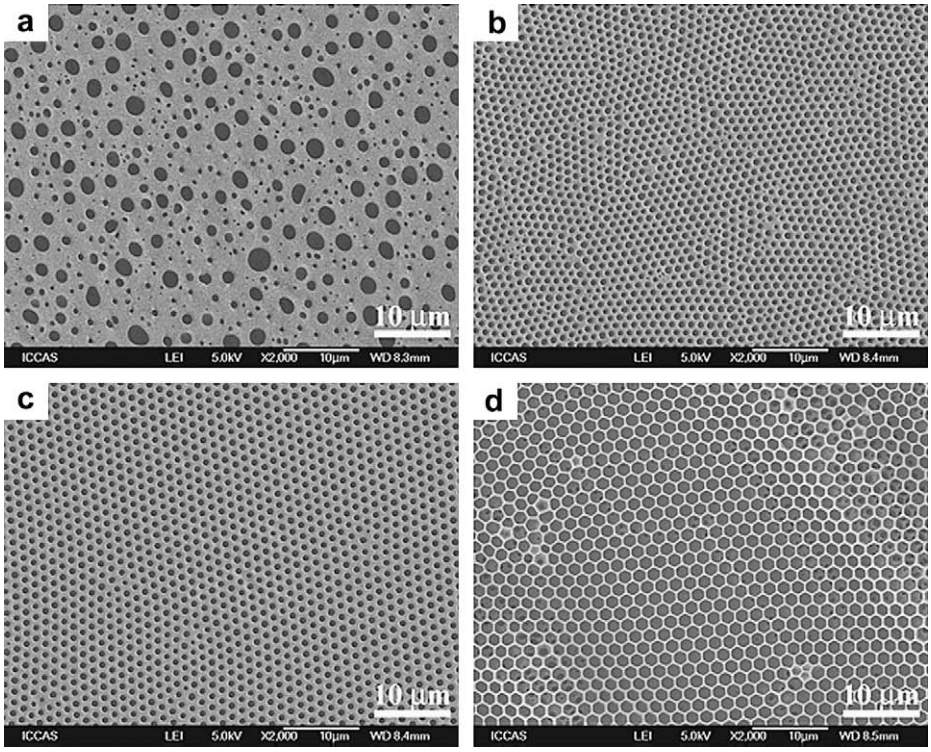

Fig. 6. SEM images of the porous films prepared from copolymer (a) $EC_{0.5}$-g-PS_{256}, (b) $EC_{0.5}$-g-PS_{162}, (c) $EC_{0.5}$-g-PS_{84}, and (d) $EC_{0.5}$-g-PS_{20} CS_2 solutions at RH of 72%. The copolymer concentration is kept at 10 g/L.

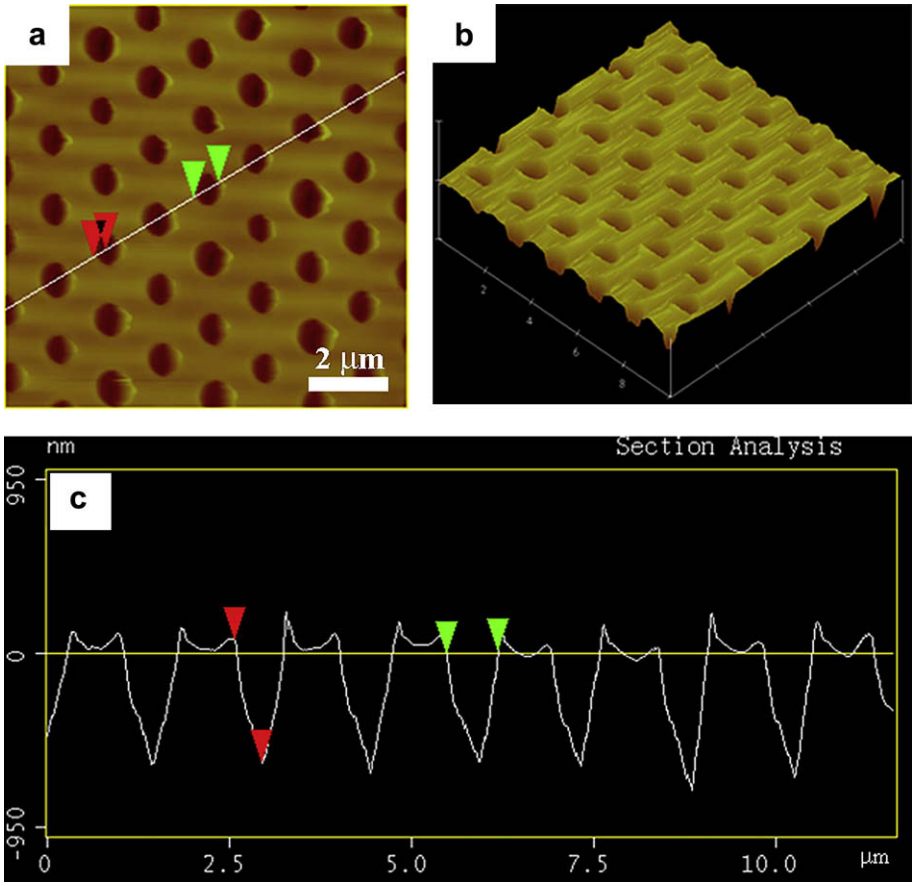

Fig. 7. AFM image (a) top view, (b) 3D view, and (c) cross-sectional analysis of the microporous film prepared from $EC_{0.5}$-g-PS_{162}/CS_2 solution with the copolymer concentration of 10 g/L at RH of 72%.

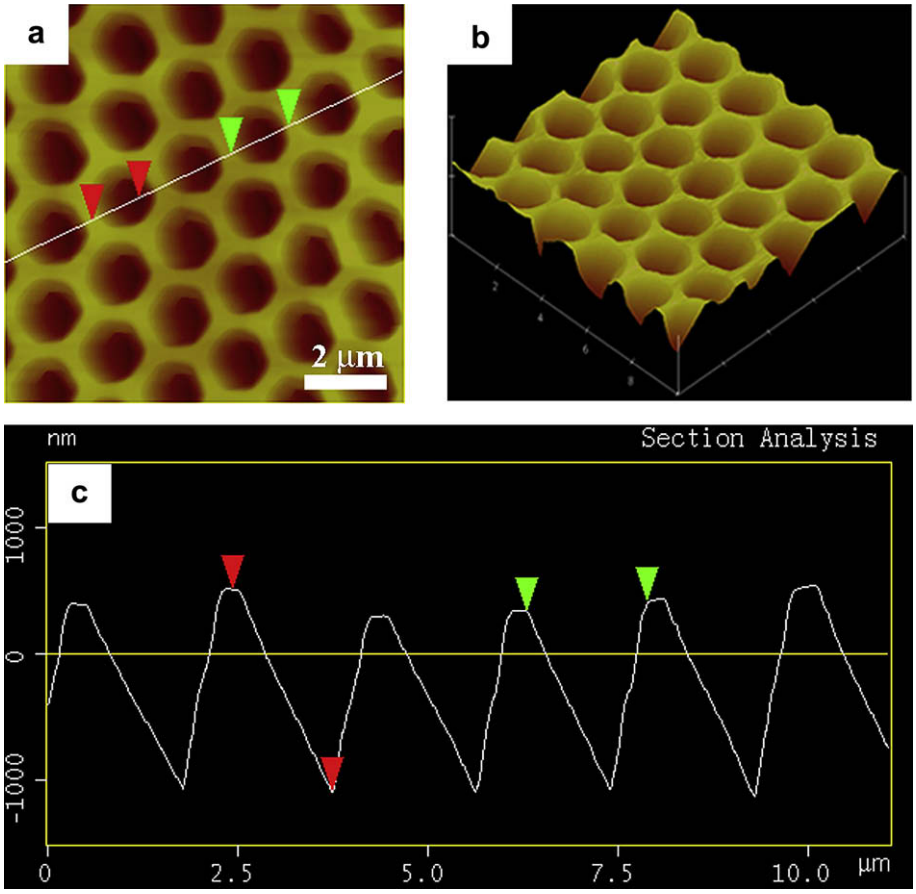

Fig. 8. AFM image (a) top view, (b) 3D view, and (c) cross-sectional analysis of the microporous film prepared from $EC_{0.5}$-g-PS_{20}/CS_2 solution with the copolymer concentration of 10 g/L at RH of 72%.

AFM section analysis, it was found that the average pore depth remained constant at about 800 nm at the polymer concentration of 5, 10, and 15 g/L (Fig. 5a–c), while that was only about 60 nm at the polymer concentration of 20 g/L (Fig. 5d). The deep pore from polymer solution with concentration of 5, 10, and 15 g/L indicated the water droplets sank into the solution surface, while the shallow pore from polymer solution with high concentration of 20 g/L implied the droplets just stayed onto the solution surface.

In the process of preparing ordered microporous film by the breath figure method, the water droplets act as the template. Therefore, the pore size is determined by the sizes of the condensed water droplets. The formation process of water droplets in breath figure method includes the nucleation and growth steps [16], which relates to the vapor pressure and the depression of the surface temperature due to the solvent evaporation. Generally,

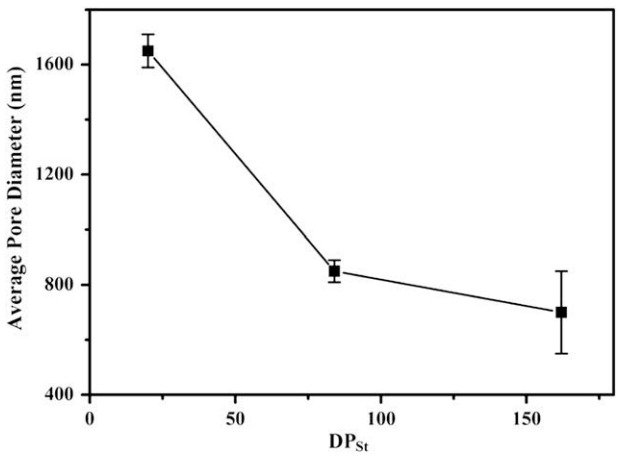

Fig. 9. The average pore size as a function of side PS chain length (DP_{st}) of the porous films prepared from EC-g-PS/CS_2 solutions with the copolymer concentration of 10 g/L at RH of 72%.

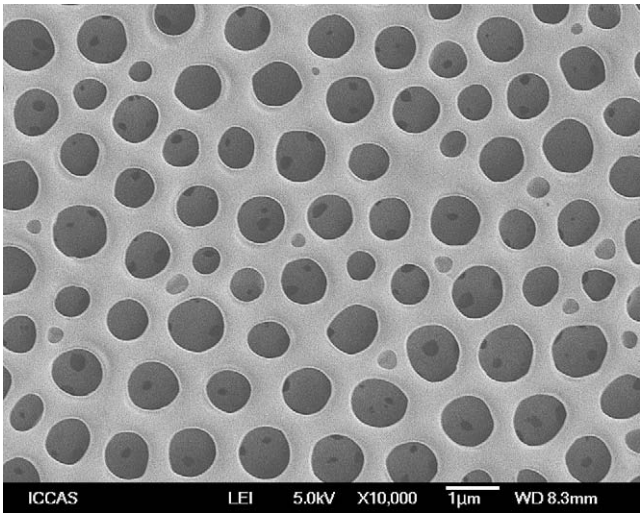

Fig. 10. Typical SEM image of the microporous film prepared from $EC_{0.5}$-g-PS_{84}/CH_2Cl_2 solution with the copolymer concentration of 10 g/L at RH of 72%.

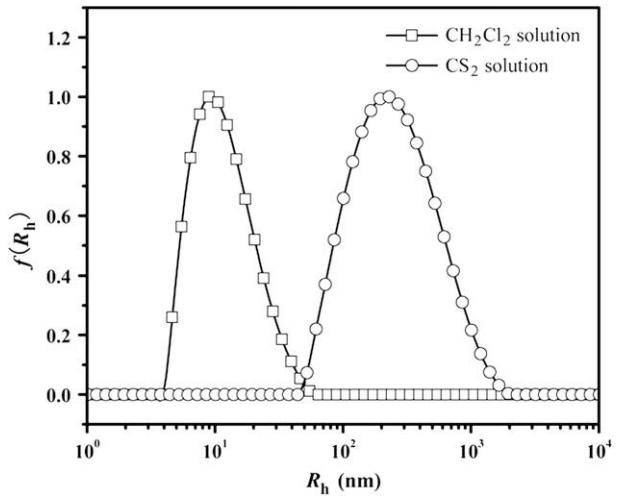

Fig. 11. Hydrodynamic radius distribution of $EC_{0.5}$-*g*-PS_{84} in CS_2 and CH_2Cl_2. The copolymer concentration is 10 g/L.

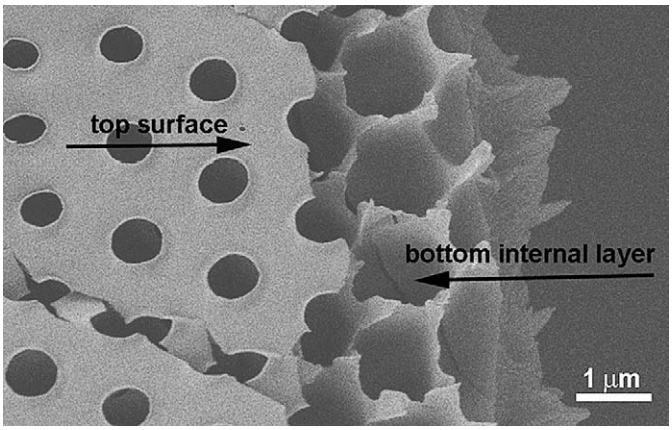

Fig. 13. SEM image of the surface and internal morphology of the film prepared from the $EC_{0.5}$-*g*-PS_{84}/CS_2 solution with a copolymer concentration of 15 g/L at RH of 72%.

a high polymer concentration corresponds to a low vapor pressure at the surface of the solution and a slow evaporation rate of the solvent, which leads to a small depression of the surface temperature ΔT ($=T_a - T_s$, where T_a and T_s are the temperatures of the atmosphere and the solution surface, respectively). At the nucleation stage of water droplets, a solution with high concentration corresponds to a smaller ΔT. It has been reported that the growing rate of the water droplets in figure breath method dR/dt relates to ΔT as $dR/dt \sim \Delta T^{0.8}$, where R is the radius of the droplets [66]. Therefore, the growing rate of the water droplets on the surface of the solution with a higher polymer concentration is slower and the obtained water droplets have a smaller size as a result, which leads to a smaller pore size. On the other hand, as mentioned above, the precipitation rate is the key factor for the formation of order patterned film. Generally, the higher polymer concentration leads to the faster precipitation of the polymer, by which the water droplets could be encapsulated and solidified immediately. Moreover, higher polymer concentration corresponds to the higher viscosity and leads to an increased efficiency of encapsulation of condensed water droplets. Therefore, the droplets do not have enough time to grow larger [29,59,67] and small pores are formed as a result. However, at the excessively low polymer concentration, e.g. 1 g/L in this work (Fig. 2a), porous films with disordered arrangement were obtained, which is due to that the viscosity of the solution is too low to stabilize the water droplets or prevent their coalescence. With the increase in polymer concentration, the water droplets can be stabilized by the solution, which is in favor of arraying the droplets orderly and forming the ordered porous structure (Fig. 2b–e). On the other hand, when the concentration is too high, the resulting viscosity would be too high to prevent the condensed water droplets from sinking into the solution surface, and the droplets could be solidified immediately and have enough time to array orderly, resulting in the disordered small pore size with shallow depth (Fig. 2f and Fig. 5d).) These results suggest that a suitable polymer concentration is needed for the formation of the ordered porous structure. Therefore, in this work, the pore size of the porous film can be adjusted by tuning the concentration of the graft copolymers. The obtained films can be used as the templates and scaffolds for the preparing of the ordered microstructure. Moreover, the porous size of the obtained film is in the range of the wavelength of visible light, which leads the potential applications in field of optical and photonic materials.

With the successes in the controlled living polymerization such as ATRP, cellulose copolymers with well-defined architecture have been prepared in our group [52–55]. Fig. 6 shows the SEM images of the microporous films prepared from the solutions of EC-*g*-PS copolymers with different side chain length (DP_{St}). The copolymer concentration in CS_2 solutions was set at 10 g/L and the RH was set at 72%. The details of the EC-*g*-PS copolymers are listed in Table 1. In the case of the copolymer with the longest side chain, $EC_{0.5}$-*g*-PS_{256} ($DP_{st} = 256$), the disordered porous film can be obtained and the pore size has a wide distribution. The relative ordered structure could be obtained from the copolymer $EC_{0.5}$-*g*-PS_{162} with relative shorter side chain ($DP_{st} = 162$) than that of copolymer $EC_{0.5}$-*g*-PS_{256}

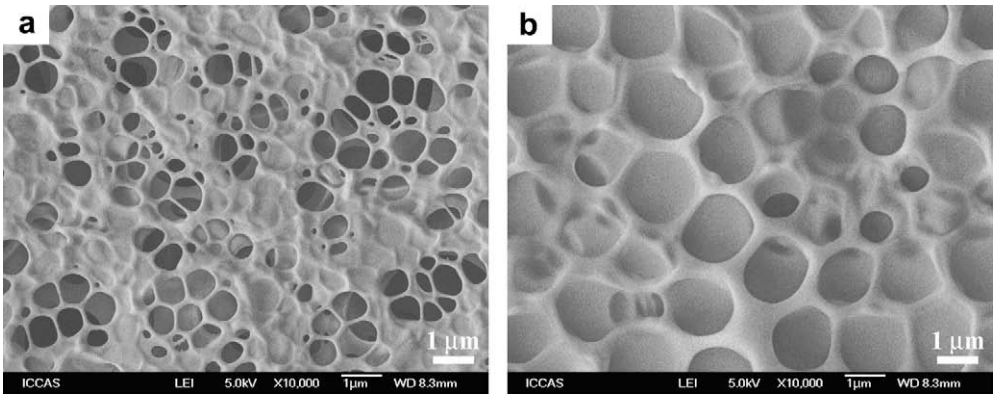

Fig. 12. SEM images of the films prepared from (a) $EC_{0.5}$-*g*-$PtBA_{53}$/CS_2 and (b) $EC_{0.02}$-*g*-$P(PEGMA)_{57}$/CH_2Cl_2 solutions at RH of 72%. The copolymer concentration is 10 g/L.

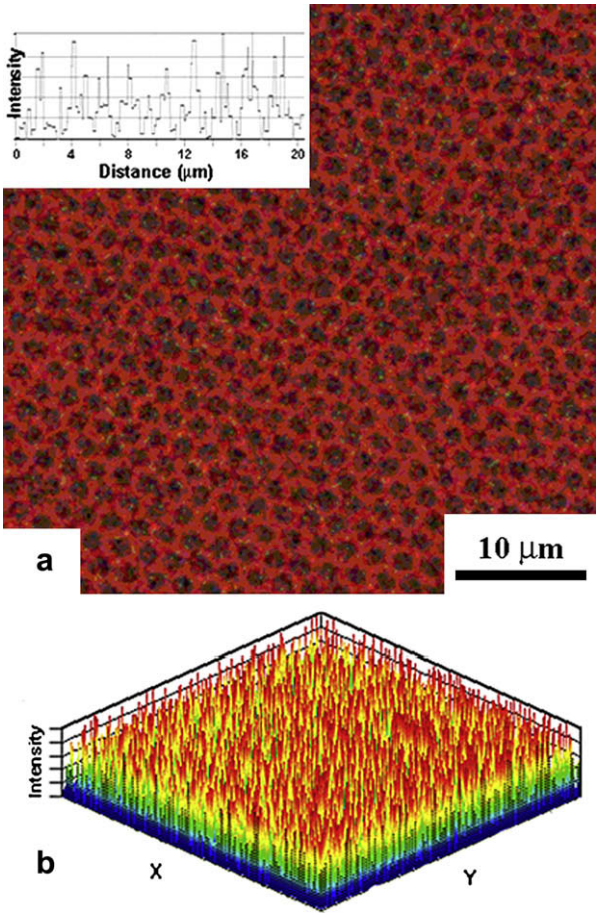

Fig. 14. Fluorescence images of the hybrid microstructure films (a) and 3D intensity distribution (b).

and the average diameter of pore is about 700 nm, which was also confirmed by AFM (Fig. 7). Specifically, hexagonal pore morphology was observed (Fig. 6d) in the film prepared from the copolymer $EC_{0.5}$-*g*-PS_{20} with the shortest side chain ($DP_{st} = 20$), which is different from the circular pores in the films prepared from copolymer $EC_{0.5}$-*g*-PS_{256}, $EC_{0.5}$-*g*-PS162, and $EC_{0.5}$-*g*-PS_{84}. The micropores are well arranged and the pores have an average size of 1.65 μm. The AFM results further confirmed the hexagonal pore as shown in Fig. 8. The dependence of the pore size on the side chain length is depicted in Fig. 9. The results indicate that the average pore size is decreased with increasing side chain length under the similar preparation conditions. Our results are different from those of linear, star, and comb PS copolymers with hydrophilic tail, core, and backbone, respectively [25–27], in which the pore size is increased with the increase in the molecular weight. The difference may be due to that EC backbone is hydrophobic for our copolymers.

The influences of the molecular weight (M_w) on the pore size of the film prepared by the breath figure method have been reported in recent years [58]. Generally, the increase in M_w leads to a larger pore size. It is believed that the higher M_w means lower mole fraction and a faster solvent evaporation, which is beneficial for the growth of the condensed water droplets [59]. In present work, the increase in the side chain length corresponds to the increase in M_w. Similar to those used the higher M_w polymers, EC-*g*-PS copolymer with a long side chain corresponds to the higher viscosity of the copolymer solution, which prevents the sinking of the water droplets into the solution surface and is not beneficial for the ordered arrangement of water droplets. Therefore, ordered films cannot be prepared by using copolymer $EC_{0.5}$-*g*-PS_{256} that has the longest side chain. However, in present work, the pore size was decreased with increasing the side chain length. This is due to that the shorter the graft chain corresponds to the lower precipitation rate, which leads to the delayed enveloping of the water droplets and the lagged solidifying of the copolymer in the surrounding solution. The continuous growth of water droplets resulted in the formation of hexagonal pore. The results mentioned above suggest that the honeycomb films with controllable pore size and pore morphology can be prepared by tuning the graft side chain length.

Solvent is the other important factor for the formation of the ordered microstructure. The effect of the solvent on the porous film has been intensively discussed [33,58]. Different solvent is normally needed when different polymers were used for the preparation of the porous films by breath figure method. As discussed above, the evaporation rate of the solvent is one of the key factors for the formation of the porous structures. Fast evaporation solvent rate corresponds to the rapid cooling rate of the surface of the polymer solution and favors condensing of water vapor. In present work, carbon disulfide (CS_2), dichloromethane (CH_2Cl_2), and toluene, which were different in vapor pressure and molecular weights, were used to investigate the influence of solvent on the porous films. Copolymer $EC_{0.5}$-*g*-PS_{84} was used and the concentration of the solution was kept at 10 g/L. All the experiments were carried out at RH = 72%. In general, higher vapor pressure and lower molecular weight lead to the faster evaporation of the solvent. Therefore, the volatilization of toluene is much slower than both CS_2 and CH_2Cl_2, while the later two solvents have almost the similar volatilization. When toluene was used as the solvent, only transparent films can be obtained, which indicated that the water vapor condensation and emulsification did not occur during the evaporation of toluene. The obtained transparent films have only a few porous structures, which are similar to those films prepared from CS_2 solvent at RH of 30%. In the case of CH_2Cl_2 and CS_2 were used as the solvent, white films were obtained. The typical SEM image shows that disordered arranged microporous films can be obtained from CH_2Cl_2 solution (Fig. 10), which is different from those ordered microporous films prepared from CS_2 solution under the same condition. The different structure in films prepared from CS_2 and CH_2Cl_2 is may be due to that CS_2 is a non-solvent of the EC backbone of the copolymer and CH_2Cl_2 is a good solvent of the EC main chain. DLS experiments also indicate that copolymer $EC_{0.5}$-*g*-PS_{84} can self-assemble into aggregates with a hydrodynamic radius (R_h) of around 200 nm, whereas the copolymers are in their single molecular state in CH_2Cl_2 with an R_h of about 10 nm (Fig. 11). The above results indicate that a selective volatile solvent is necessary for ordered arrangement in breath figure method for our system. The self-assembly of the graft copolymer in the selective solvent is beneficial for the formation of well-arranged microporous films, as reported in previous work [18,68].

In order to further confirm the influence of precipitation rate on the morphology of the microporous films by breath figure method, the other ethyl cellulose graft copolymers, $EC_{0.5}$-*g*-$PtBA_{53}$ and $EC_{0.02}$-*g*-$P(PEGMA)_{57}$, were used. Because of the low temperature of glass, PtBA should be correlated with a slow precipitation around condensed water droplets. The hydrophilic P(PEGMA) side chains should also correspond to a slower precipitation rate around condensed water droplets because of their hydrophilicity. However, no ordered microporous film can be obtained from the copolymer $EC_{0.5}$-*g*-$PtBA_{53}$/CS_2 solution and $EC_{0.02}$-*g*-$P(PEGMA)_{57}$/CH_2Cl_2 solution (Fig. 12), which confirms that the precipitation rate of the copolymer is one of the key factors for the preparation of microporous films by breath figure approach and timely precipitation is required to obtain highly ordered porous films. The larger hole in the film from the $EC_{0.02}$-*g*-$P(PEGMA)_{57}$ copolymer also indicated that the $EC_{0.02}$-*g*-$P(PEGMA)_{57}$ copolymer has the poorer ability to envelope and freeze the condensed water droplets because of its

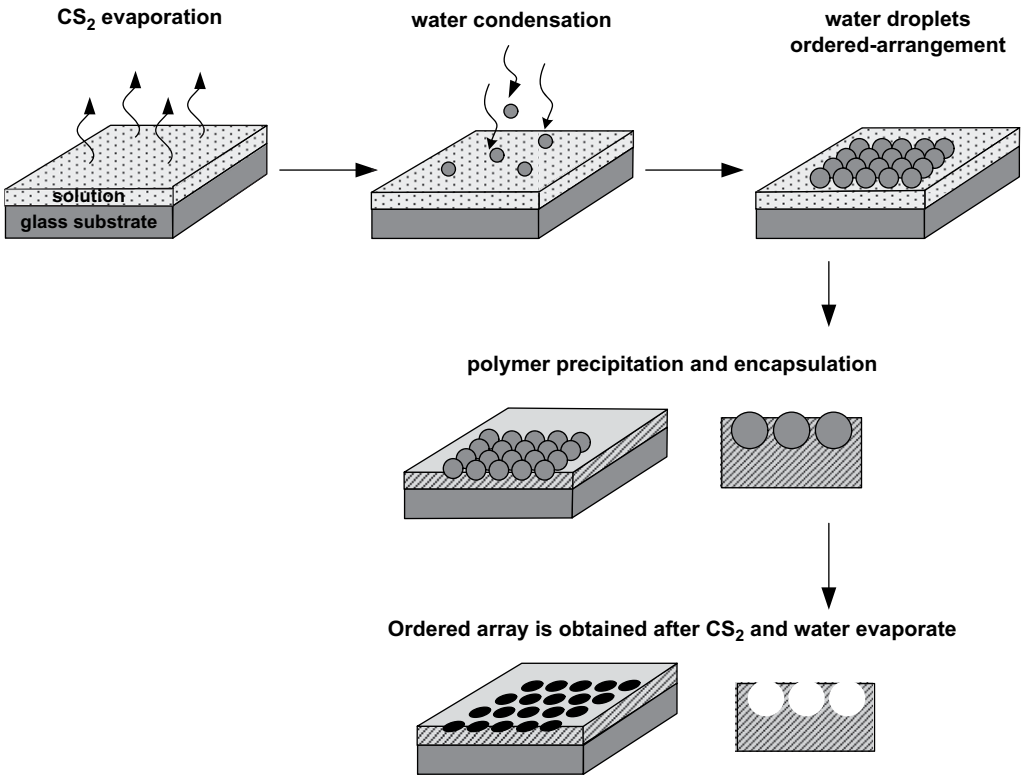

Fig. 15. Scheme of the mechanism of the formation of the honeycomb EC-*g*-PS films on a substrate by breath figure approach.

strong hydrophilicity. The results suggested that the hydrophobic side chain with fast precipitation rate is of importance in the process of porous self-organization.

Fig. 13 shows the internal morphology of the obtained films from copolymer $EC_{0.5}$-*g*-PS_{84} at 15 g/L solution concentration and 72% RH, which indicate that the hole size on the surface is smaller than that of the internal. The pore structure could be of interest in nano- and microcontainer-type applications. The ordered patterned films with good spatial array could be used to fabricate the functional films by simple hybrid of copolymer and functional materials. If the fluorescence dye is added, fluorescent films with regular fluorescence emission intensity can be obtained as shown in Fig. 14. It can be seen that morphology of the film is well preserved and the dye dispersed according the morphology of the film. Moreover, the fluorescence intensity profile of the microporous films is in the regular pattern (Fig. 10a, inset). The fluorescence intensity distributes according to the arrangement of the pore on the film (Fig. 10b). Similar honeycomb patterned photo-luminescent films have been successively prepared from hyperbranched poly(amidoamine)s (HPAMAMs) [69]. The dye hybrid films can be used as electronic devices and have other potential applications in the fields of photonic and bandgap materials [65,70,71].

The mechanism of the ordered microporous structures from the cellulose-based graft copolymers by breath figure method can be depicted schematically in Fig. 15. The rapid evaporation of CS_2 leads to the rapid cooling of the solution surface and the condensation of the water vapor in the moist atmosphere onto the surface of the film, which results formation of the water microdroplets on the surface by the nucleation and growth of the water vapor [16]. Both the capillary attractive forces and the convection currents due to evaporation drive the ordered hexagonal packing of the water droplets with the simultaneously precipitation of the copolymer at the water-solution intersurface [72,73]. The ordered microporous films can be obtained after dried the film.

4. Conclusion

The ordered porous honeycomb films were successfully prepared from cellulose-based graft copolymers by breath figure method. The influences of the RH, copolymer concentration, graft side chain length, the solvents, and the type of graft side chain on the morphology obtained were investigated. It was found that a suitable copolymer concentration, the length of the side chain, and comparably high RH are needed for the ordered formation. The range of pore size could be tailored from 100 nm to 2 μm by varying the copolymer concentration or graft side chain length. The ordered arrays are the result of self-organized water droplets, which act as the templates in the formation process. Moreover, it was confirmed that the aggregation of the graft copolymer was beneficial for the ordered patterns. The precipitation of polymer is a key factor and the precipitation rate play an important role in forming the ordered porous structures, which was further confirmed by comparison of type of graft side chain. Furthermore, the preliminary studies on hybrid films with fluorescence dye demonstrated the good ability of the honeycomb films as templating, which could be extended for other functional materials. Anyway, the porous honeycomb films are interesting as templates, nanocontainer and photonic band gaps because of their order and their size comparable to the wavelength of visible light.

Acknowledgement

The financial supports of National Natural Science Foundation of China (Grant No. 50821062, 20774105) and Chinese Academy of Sciences (Grant No. KJCX2-SW-H07) are greatly appreciated.

References

[1] Hulteen JC, Jirage KB, Martin CR. J Am Chem Soc 1998;120:6603.
[2] de Boer B, Stalmach U, Nijland H, Hadziioannou G. Adv Mater 2000;12:1581.
[3] Yabu H, Shimomura M. Langmuir 2005;21:1709.
[4] Beattie D, Wong KH, Williams C, Poole-Warren LA, Davis TP, Barner-Kowollik C, et al. Biomacromolecules 2006;7:1072.
[5] de Boer B, Stalmach U, Melzer C, Hadziioannou G. Synth Met 2001;121:1541.
[6] Yabu H, Takebayashi M, Tanaka M, Shimomura M. Langmuir 2005;21:3235.
[7] Fukuhira Y, Kitazono E, Hayashi T, Kaneko H, Tanaka M, Shimomura M, et al. Biomaterials 2006;27:1797.
[8] Yabu H, Shimomura M. Chem Mater 2005;17:5231.
[9] Sun ZQ, Li YF, Wang YF, Chen X, Zhang JH, Zhang K, et al. Langmuir 2007;23:10725.
[10] Gates B, Yin YD, Xia YN. Chem Mater 1999;11:2827.
[11] Imhof A, Pine DJ. Nature 1997;389:948.
[12] Davis SA, Burkett SL, Mendelson NH, Mann S. Nature 1997;385:420.
[13] Hoa MLK, Lu MH, Zhang Y. Adv Colloid Interface Sci 2006;121:9.
[14] Bunz UHF. Adv Mater 2006;18:973.
[15] Jenekhe SA, Chen XL. Science 1999;283:372.
[16] Srinivasarao M, Collings D, Philips A, Patel S. Science 2001;292:79.
[17] Ishizu K, Tokuno Y, Makino M. Macromolecules 2007;40:763.
[18] Widawski G, Rawiso M, Francois B. Nature 1994;369:387.
[19] Francois B, Pitois O, Francois J. Adv Mater 1995;7:1041.
[20] Lord HT, Quinn JF, Angus SD, Whittaker MR, Stenzel MH, Davis TP. J Mater Chem 2003;13:2819.
[21] Song L, Bly RK, Wilson JN, Bakbak S, Park JO, Srinivasarao M, et al. Adv Mater 2004;16:115.
[22] Pitois O, Francois B. Colloid Polym Sci 1999;277:574.
[23] Yabu H, Tanaka M, Ijiro K, Shimomura M. Langmuir 2003;19:6297.
[24] Stenzel MH. Aust J Chem 2002;55:239.
[25] Stenzel MH, Davis TP, Fane AG. J Mater Chem 2003;13:2090.
[26] Stenzel-Rosenbaum MH, Davis TP, Fane AG, Chen V. Angew Chem Int Ed 2001;40:3428.
[27] Stenzel MH, Barner-Kowollik C, Davis TP. J Polym Sci Part A Polym Chem 2006;44:2363.
[28] Cheng CX, Tian Y, Shi YQ, Tang RP, Xi F. Langmuir 2005;21:6576.
[29] Zhao BH, Zhang J, Wang XD, Li CX. J Mater Chem 2006;16:509.
[30] Karikari AS, Williams SR, Heisey CL, Rawlett AM, Long TE. Langmuir 2006;22:9687.
[31] Cheng CX, Tian Y, Shi YQ, Tang RP, Xi F. Macromol Rapid Commun 2005;26:1266.
[32] Tian Y, Liu S, Ding HY, Wang LH, Liu BQ, Shi YQ. Polymer 2007;48:2338.
[33] Tian Y, Jiao QZ, Ding HY, Shi YQ, Liu BQ. Polymer 2006;47:3866.
[34] Zhao B, Li CX, Lu Y, Wang XD, Liu ZL, Zhang BH. Polymer 2005;46:9508.
[35] Wong KH, Davis TP, Bamer-Kowollik C, Stenzel MH. Polymer 2007;48:4950.
[36] Lin CL, Tung PH, Chang FC. Polymer 2005;46:9304.
[37] Cui L, Peng J, Ding Y, Li X, Han YC. Polymer 2005;46:5334.
[38] Maruyama N, Koito T, Nishida J, Sawadaishi T, Cieren X, Ijiro K, et al. Thin Solid Films 1998;329:854.
[39] Yamamoto S, Tanaka M, Sunami H, Ito E, Yamashita S, Morita Y, et al. Langmuir 2007;23:8114.
[40] Nishida J, Nishikawa KA, Nishimura S, Wada S, Karino T, Nishikawa T, et al. Polym J 2002;34:166.
[41] Liang SM, Zhang L, Xu H. J Membr Sci 2007;287:19.
[42] Kasai W, Kondo T. Macromol Biosci 2004;4:17.
[43] Park MS, Joo W, Kim JK. Langmuir 2006;22:4594.
[44] Zhou JP, Zhang L, Deng QH, Wu XJ. J Polym Sci Part A Polym Chem 2004;42:5911.
[45] Cai J, Zhang LN, Zhou JP, Qi HS, Chen H, Kondo T, et al. Adv Mater 2007;19:821.
[46] Wu M, Kuga S, Huang Y. Langmuir 2008;24:10494.
[47] Roy D, Guthrie JT, Perrier S. Macromolecules 2005;38:10363.
[48] Vlcek P, Janata M, Latalova P, Kriz J, Cadova E, Toman L. Polymer 2006;47:2587.
[49] Carlmark A, Malmstrom EE. Biomacromolecules 2003;4:1740.
[50] Carlmark A, Malmstrom E. J Am Chem Soc 2002;124:900.
[51] Meng T, Gao X, Zhang J, Yuan JY, Zhang YZ, He JS. Polymer 2009;50:447.
[52] Shen DW, Yong H. Polymer 2004;45:7091.
[53] Kang HL, Liu WY, Liu RG, Huang Y. Macromol Chem Phys 2008;209:424.
[54] Kang H, Liu W, He B, Shen D, Ma L, Huang Y. Polymer 2006;47:7927.
[55] Shen DW, Yu H, Huang Y. J Polym Sci Part A Polym Chem 2005;43:4099.
[56] Li Y, Liu W, Kang H, Wu M, Liu R, Huang Y. J Polym Sci Part A Polym Chem 2008;46:6907.
[57] Liu WY, Liu RG, Li YX, Kang HL, Shen D, Wu M, et al. Polymer 2009;50:211.
[58] Peng J, Han YC, Yang YM, Li BY. Polymer 2004;45:447.
[59] Xu Y, Zhu BK, Xu YY. Polymer 2005;46:713.
[60] Tung PH, Kuo SW, Jeong KU, Cheng SZD, Huang CF, Chang FC. Macromol Rapid Commun 2007;28:271.
[61] Park MS, Kim JK. Langmuir 2004;20:5347.
[62] Li J, Peng J, Huang WH, Wu Y, Fu J, Cong Y, et al. Langmuir 2005;21:2017.
[63] Tian Y, Liu S, Ding HY, Wang LH, Liu BQ, Shi YQ. Macromol Chem Phys 2006;207:1998.
[64] Nishikawa T, Ookura R, Nishida J, Arai K, Hayashi J, Kurono N, et al. Langmuir 2002;18:5734.
[65] Barner-Kowollik C, Dalton H, Davis TP, Stenzel MH. Angew Chem Int Ed 2003;42:3664.
[66] Beysens D, Steyer A, Guenoun P, Fritter D, Knobler CM. Phase Trans 1991;31:219.
[67] Fritter D, Knobler CM, Beysens DA. Phys Rev A 1991;43:2858.
[68] Hernandez-Guerrero M, Davis TP, Barner-Kowollik C, Stenzel MH. Eur Polym J 2005;41:2264.
[69] Liu CH, Gao C, Yan DY. Angew Chem Int Ed 2007;46:4128.
[70] Busch K, John S. Phys Rev Lett 1999;83:967.
[71] Heng LP, Zhai J, Zhao Y, Xu JJ, Sheng XL, Jiang L. ChemPhysChem 2006;7:2520.
[72] Gau H, Herminghaus S. Phys Rev Lett 2000;84:4156.
[73] Limaye AV, Narhe RD, Dhote AM, Ogale SB. Phys Rev Lett 1996;76:3762.